ISSN 0024-4902, Lithology and Mineral Resources, 2017, Vol. 52, No. 6, pp. 447–466. © Pleiades Publishing, Inc., 2017.
Original Russian Text © Yu.O. Gavrilov, E.V. Shchepetova, E.A. Shcherbinina, O.V. Golovanova, R.I. Nedumov, B.G. Pokrovsky, 2017, published in Litologiya i Poleznye Iskopaemye, 2017, No. 6, pp. 503–526.

Sedimentary Environments and Geochemistry of Upper Eocene and Lower Oligocene Rocks in the Northeastern Caucasus

Yu. O. Gavrilov*, E. V. Shchepetova, E. A. Shcherbinina, O. V. Golovanova, R. I. Nedumov, and B. G. Pokrovsky

Geological Institute, Russian Academy of Sciences Pyzhevskii per, 7, Moscow, 119017 Russia

**e-mail: gavrilov@ginras.ru*

Received May 19, 2017

Abstract—Upper Eocene and Lower Oligocene rocks in the northeastern Caucasus were examined in the most representative Chirkei section (Sulak River basin). Sharp lithogeochemical distinctions between them were revealed. The results of the study of nannoplankton demonstrated that the Eocene/Oligocene interface occurs slightly below the boundary between the Belaya Glina and Khadum formations. The studied section revealed a series of nannoplankton bioevents facilitating its stratigraphic subdivision. It has been established that organic matter (OM) in rocks of the Khadum Formation is characterized by a relatively high degree of maturity. Probably, the material of mainly marine genesis contains a terrigenous OM admixture. Positive oxygen isotope anomaly in the upper part of the Belaya Glina Formation reflects global climate changes (cooling) near the Eocene/Oligocene interface. Limitation of the anomaly by the upper boundary of the Belaya Glina Formation is likely related to changes in water salinity variations in the Early Oligocene basin and intense early diagenetic processes in rocks therein. Lithological, geochemical, and paleoecological data suggest that the Khadum paleobasin was depleted in oxygen. Such environment was unstable with periodic intensification or attenuation. Paleoecology in the Belaya Glina basin was typical of normally aerated basins.

DOI: 10.1134/S0024490217060037

INTRODUCTION

Cenozoic marine sedimentary assemblages in Cis-Caucasia accommodate sequences accumulated in appreciably different sedimentation and geochemical settings—both normally aerated basins and oxygen-deficient above bottom waters. Transition of rock types between these zones is accompanied by significant changes in their lithogeochemical properties. One of the most prominent intervals is represented by the transition from rocks of the oxic Belaya Glina (Priabonian) basin to the mainly anoxic Maikop basin, more precisely, to its lower part identified as the Khadum Formation (Lower Oligocene). Comparison of these sequences unraveled the most typical features of rocks deposited in geochemically different paleobasins. The Khadum rocks are of great interest because of their high oil-generation potential.

Upper Eocene–Lower Oligocene rocks were studied in the northeastern Caucasus (Fig. 1). Here, the Sulak River basin shows the most complete section of the Maikop sequence. Based on its examination, N.S. Shatsky recognized several horizons, including the Khadum Horizon at the base (Shatsky, 1925; Shatsky and Menner, 1927). Later, numerous subsequent works addressed the stratigraphy and paleogeography of Oligocene rocks in the Caucasian region (Akhmetiev et al., 2017; *Geologicheskie* ..., 1998; Muzylev, 1992; Popov et al., 1993, 2009; Somov, 1965; Stolyarov, 1991; Stolyarov and Ivleva, 1999; Voronina and Popov, 1984; Zhizhchenko, 1958; and others). Consequently, the Khadum Horizon was divided into two units: Pshekh and Solenov. The present paper considers the Khadum sequence as a formation, which can be divided into two (Pshekh and Solenov) subformations.

The Sulak River valley exposes two sections of the Khadum Formation. The first (northern) section near the Miatly village is characterized by small thickness (about 40 m). The second (southern) section is located on the bank of the Chirkei reservoir and confined to the Chirkei depression. Here, the Khadum section is appreciably thicker (more than 250 m) and is characterized by a more complete stratigraphic volume, as noted previously by M.I. Saidov, K.I. Mikulenko, and V.F. Sharafutdinov (Sharafutdinov, 2001). Our new data on the Chirkei section, which also support this conclusion, are discussed in the present paper.

OBJECT AND METHODS

The Belaya Glina (Upper Eocene) and Khadum (Lower Oligocene) rocks were studied with various analytical methods. During their study in outcrops, we examined specific structural features of sequences and

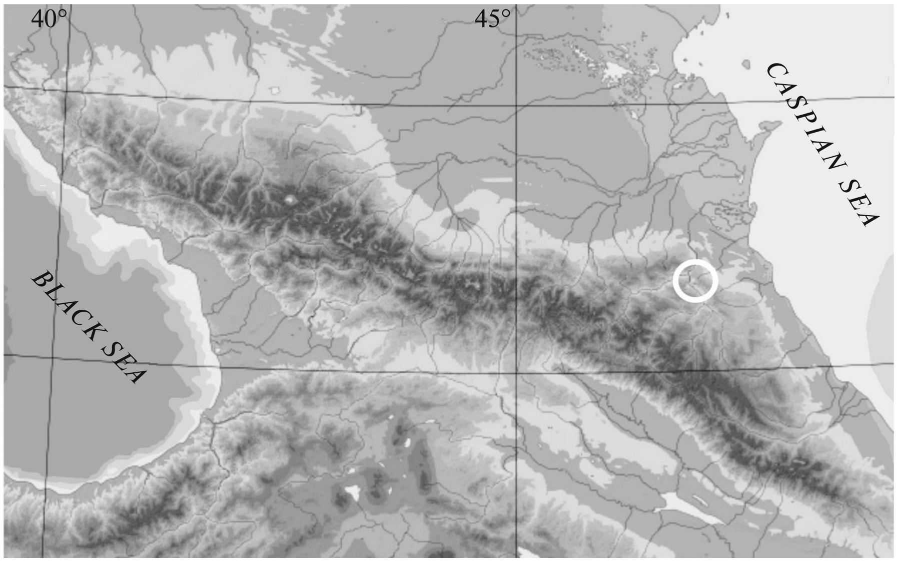

Fig. 1. Topography of the Greater Caucasus. The study area is encircled.

various properties that characterize sedimentation, cyclicity, and other features. Their laboratory examination was devoted to scrutinization of the rock composition: the content of organic carbon (C_{org}), proportion of the terrigenous and carbonate components, mineral composition of the carbonate and clayey material, distribution of different chemical elements, and behavior of carbon and oxygen isotopes.

Refinement of the stratigraphic position of formations with modern approaches and methods of biostratigraphy (study of the behavior of nannoplankton) is an important problem. Samples for studying nannoplankton were prepared from weighed rock portions according to the standard procedure (Bown and Young, 1998) using Norland Optical Adhesive 61 as the optical medium. Nannoplankton was studied under an Olympus BX41 polarization microscope, with Unfinity X videocamera for photography.

The comprehensive mineralogical-geochemical examination of rocks was accomplished in about 190 rock samples, with more than 170 analyses of the chemical composition of rocks. The analyses were carried out mostly in laboratories of the Geological Institute (Russian Academy of Sciences) using the chemical analytical, isotope geochemical and geochronological, and physical tools for the study of major minerals.

Contents of C_{org} and CO_2 were determined by the chemical analysis with a Knopp-Fresenius apparatus (*Metody* ..., 1957). The remaining elements were determined with a S4 Pioner XRF spectrometer. Data on the mineral composition of rocks were obtained with a D8 Advance (Bruker) diffractometer. The framboidal pyrite was examined with an MV 2300 scanning electron microscope equipped with INCA energy 200 EDX system. The carbon and oxygen isotopic compositions in carbonates were determined with Thermoelectron Corporation equipment system including Delta V Advantage mass spectrometer and Gas-Bench-II device. Decomposition of samples along with KH-2, IAEA C-O-1, and NBS-19 standards was accomplished with 100% H_3PO_4 at 50°C. Values of $\delta^{13}C$ and $\delta^{18}O$ are given in per mille (‰) relative to standard V-PDB, with the accuracy (reproducibility) of $\delta^{18}O$ and $\delta^{13}C$ determination at ±0.2‰ and ±0.1‰, respectively. Pyrolitic analysis of organic matter (OM) was carried out with different Rock-Eval modifications.

STRATIGRAPHIC DIVISION OF UPPER EOCENE AND LOWER OLIGOCENE ROCKS BASED ON NANNOPLANKTON

Nannoplankton was studied in the lower 80-m-thick sequence of the sampled part of the section (Belaya Glina Formation–bottom of the Solenov Subformation, Fig. 2). This part is characterized by the presence of different concentrations of calcium carbonate. The upper, certainly noncarbonate part, of the Solenov Subformation is unsuitable for studying nannoplankton.

Nannoplankton assemblages in the studied interval show appreciable variations in population, species diversity, and preservation grade. Assemblages of the Belaya Glina Formation are mainly distinguished by a low species diversity that slightly increases at some levels (Table 1, Fig. 3), relatively high total population, and sufficiently poor preservation. In the lower part of the Khadum Formation, the total nannoplankton population is slightly lower, but the preservation is notably higher. Nannoplankton assemblages in the Chirkei section are marked by appreciably lower *Dis-*

coaster abundance, probably, because of a rather intense recrystallization of carbonate-rich rocks of the Belaya Glina Formation. In rocks of the Khadum Formation, the low content of these warm water species is likely related to climate cooling in the Early Oligocene. In addition, the studied interval is rather depleted in *Reticulofenestra* spp., which is usually abundant in the Late Eocene nannoplankton assemblages. At the same time, virtually the entire section is dominated by the consanguineous *Dictyococcites*. Extreme rarity of species of the coldwater *Chiasmolithus*, which are highly recrystallization-resistant, suggests their initial low population.

The series of nannoplankton bioevents deciphered in the section makes it possible to define stratigraphic subdivision based on three scales proposed by E. Martini (Martini, 1971), H. Okada and D. Bukry (Okada and Bukry, 1980), and C. Agnini and coauthors (Agnini et al., 2014) that are coded as NP, CP, and CNE/CNO, respectively. However, the lack or extreme rarity of some stratigraphically important species in the section hampers the identification of some zonal subdivisions.

The presence of rare *Chiasmolithus oamaruensis* and *Isthmolithus recurvus* at the base of the Belaya Glina Formation makes it possible to define Upper Eocene zones NP19 and CP15. Complexity of the zonal division of the Late Eocene based on NP and CP scales was repeatedly discussed in (Agnini et al., 2014; Costa et al., 2013; Cotton et al., 2017; Fornaciari et al., 2010; Strougo et al., 2013). The first occurrence (FO) of *Isthmolithus recurvus* is used in these scales to define the lower boundaries of zone NP19-20 and subzone CP15b. However, earlier occurrence of rare specimens of this species in the Middle Eocene rocks in some sections considerably hampers the determination of these boundaries. In (Agnini et al., 2014), the first level of the constant presence of this species (Base common) was proposed to accept as the most reasonable marker. However, the Chirkei section only contains sporadic specimens of this species in the Upper Eocene rocks, whereas their constant presence is recorded in the Lower Oligocene part of the Maikop Group (Pshekh Subformation). In addition, this section is marked by extreme rarity of the rosette-shaped *Discoaster* species (*Discoaster saipanensis* and *D. barbadiensis* with a similar disappearance level), whose disappearance marked the base of zones NP16, CP21, and CNE21 in the terminal part of the Late Eocene, does not make it possible to recognize these subdivisions.

The first occurrence of *Cribrocentrum isabellae* at the level of 12 m (sample 204) records the base of zone CNE19, whereas the last occurrence (LO) of *C. reticulatum* 20 m upward records the base of zone CNE20. Beginning of the interval of high population (acme) of *Clausicoccus subdistichus*, which is considered at present as the closest one to the Eocene/ Oligocene inter-

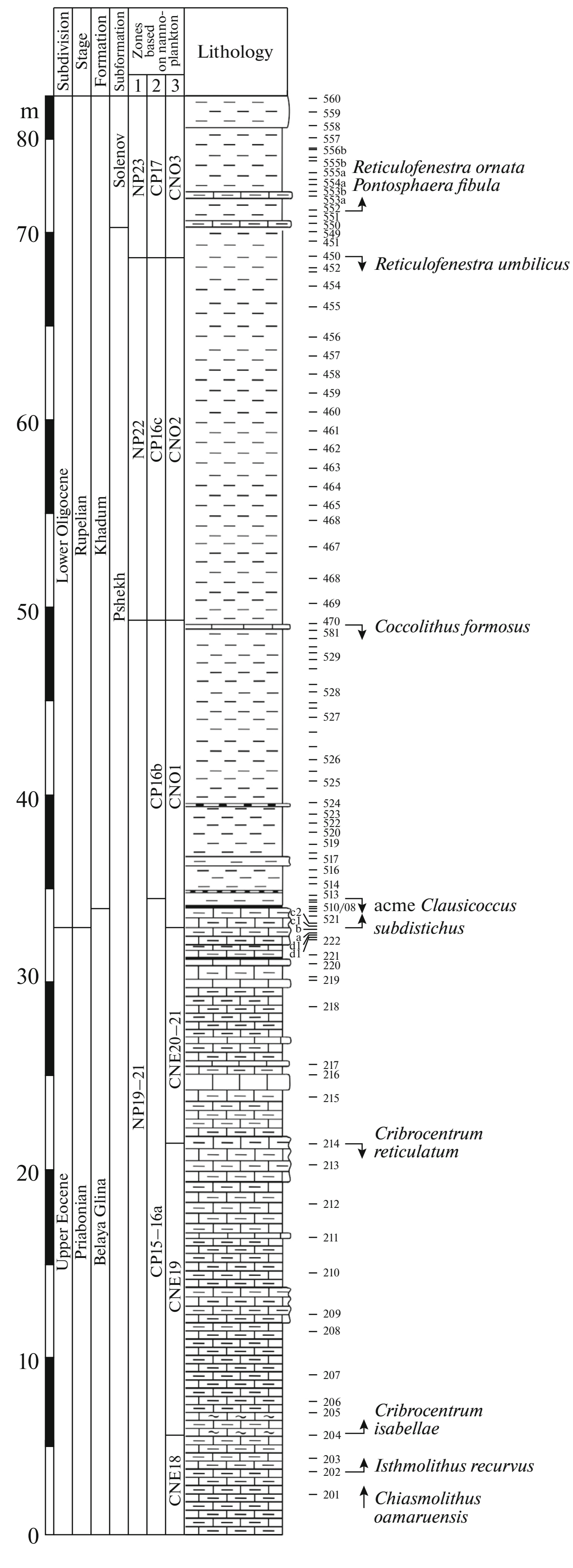

Fig. 2. Lithological structure, stratigraphic subdivision and most significant events in the nannoplankton composition of assemblages of the Belaya Glina Formation and lower part of Maikop Group (Pshekh and Solenov subformations) in the Chirkei section.

Table 1. Population and stratigraphic distribution of nannoplankton in Upper Eocene and Lower Oligocene sediments in the Chirkei section

Upper Eocene																									Lower Oligocene					Subdivision
Priabonian																									Rupelian					Stage
Belaya Glina																											Pshekh			Formation
NP20–NP21																														zones based on nannoplankton: Martini, 1971
CP15–CP16a																												CP16b		zones based on nannoplankton: Okada, Bukry, 1980
CNE18			CNE19											CNE20–CNE21											CNO1					zones based on nannoplankton: Agnini et al., 2014
201	202	203	204	205	206	207	208	209	210	211	212	213	214	215	216	217	218	219	220	222	d1	d2	a	b	c1	c2	510	511	512	sample no. / nannoplankton species
f	f	f		f			f	f	r	r	r	f	f	f	r	f	f	f	r		f			f	f		f	f	r	*Bicolumnus ovatus*
f		f			f		f	f	f	f	f	f	f	f			f		r	r	f					f	r	f	f	*Blackites spinosus*
f										f		f			f			f												*Chiasmolithus oamaruensis*
c	r	c	r	r	r	f	f	f	r	r	r	c	c	c	c	c	c	r	c	r	c	r	r	r	r	f	f	f	f	*Coccolithus formosus*
r	r	r	r	r	c	c	c	c	c	c	c	c	c	c	c	c	c	r	r	r	c	c	c	r	c	r	r	r	r	*C. pelagicus*
r	r	f	r	f	r	f	f	f	f	f	f	r	f		f			f	f							f				*Cribrocentrum erbae*
f	f							f	f		f	f	f																	*C. reticulatum*
c	r	c	c	c	c	c	c	c	c	c	r	r	c	c	c	c	a	r	c	c	c	c	r	c	c	c	a	a	a	*Cyclycargolithus floridanus*
c	r	f	f	f	r	r	a	c	a	a	a	r	c	a	c	c	c	c	a	c	c	r	c	c			c	c	c	*Dictyococcites bisectus*
a	c	c	r	r	r	r	c	c	r	r	r	f	f	f	r	f	r	f	f	f					f	f	r	r	f	*D. scrippsae*
f																														*Discoaster barbadiensis*
f							f										f					f					f	f		*Helicosphaera bramlettei*
f	r	r	c	c	c	c	f	f	f	f	f		f				f	r	r	r	f	f	f	f	f			f	f	*Lanternithes minutus*
f	f	f						f	f	f	f	f				f	f	f		f				f	f	f				*Reticulofenestra dictyoda*
f			f			f	f	f	r	f	f	f	f	f	f	f	f	f	f			f	f		f		f			*R. hillae*
f	f	f	f	f	f	r	f	f	f	f	r	r	r	c	r	c	r	f	f	f	r	f	r	r	r	f	f	r	r	*R. umbilicus*
c	r	c	c	c	c	r	r	r	c	c	c	c	r	r	r	r	r	r	f	f	r	r	r	f	r	f	r	r	r	*Sphenolithus moriformis*
f				f				f	f	f	f	f												f						*Sphenolithus pseudoradians*
f	r	c	r	c	r	r	r	f	f	f	f	f				f	r	f		f		f		f	r		f	r	r	*Zygrhablithus bijugatus*
	f				f				f	f			f			f	f		f								f		f	*Isthmolithus recurvus*
			f		f	f		f		f				f	f	f	f	f				f		f	f					*Blackites tenuis*
			r	f	f	f	f	f	f	f	f			f	f															*Cribrocentrum isabellae*
				f		f											f			f	f	f	f	f	r	r	c	r	f	*Clausicoccus subdistichus*
					f	f	f																							*Umbilicosphaera protoannulus*
						f						f																		*Discoaster saipanensis*
							f																	f						*Chiasmolithus altus*
							f										f													*Helicosphaera compacta*
															f	r	f		f		f						f			*Discoaster nodifer*
															f		f		f									f		*D. tani*
																f											f			*D. deflandrei*
																	f								f	f				*Reticulofenestra lockeri*
																	f	f												*Helicosphaera* sp. 3 Bown, 2005
																		f		f										*Pontosphaera plana*

Table 1. (Contd.)

Lower Oligocene																						Subdivision
Rupelian																						Stage
Pshekh																	Solenov					Formation
NP19–21									NP22								NP23					zones based on nanno-plankton: Martini, 1971
CP16b									CP16c								CP17					zones based on nanno-plankton: Okada, Bukry, 1980
CNO1									CNO2								CNO3					zones based on nanno-plankton: Agnini et al., 2014
513	514	515	516	518	519	520	530	470	469	468	467	466	465	464	463	462	549	552	553a	553b	554a	sample no. / nanno-plankton species
f				f	f				f	f	f			f								*Blackites spinosus*
f			f	f	f	f		f														*Coccolithus formosus*
r	f	f	f	f	f	f	r	f	r	r	r	r	r	r	r	f		f	f		f	*C. pelagicus*
f			f																	f	f	*Cribrocentrum erbae*
c	r	r	f	f	r	r	r	r	r	f	f	f	f	f	f	f	f	f	f	f	f	*Cyclycargolithus floridanus*
c	f	f		f	r		c	r	c	c	r	r	r	r	f	r	f	f	f		f	*Dictyococcites bisectus*
f			f	f					f					f				f	f			*D. scrippsae*
f				f			f	f			f		f								f	*Lanternithes minutus*
f				f					f	f	f	f				f			f		f	*Reticulofenestra dictyoda*
f	f			f	f	f	f		f	f	f	f	f	f	f	f						*R. umbilicus*
r	f	f			f	r				f						f						*Sphenolithus moriformis*
r			f	f	f	r	r		f		f		f	f						f		*Zygrhablithus bijugatus*
				f	f																	*Clausicoccus subdistichus*
					f																	*Discoaster nodifer*
								f	f													*Bicolumnus ovatus*
								f			f				f							*Helicosphaera compacta*
										f	f								f		f	*Reticulofenestra circus*
																		f	f		f	*Pontosphaera fibula*
																		f	r	f		*Reticulofenestra ornata*
																			f	f	f	*R. lockeri*

(a) abundant (>5 specimens in the microscopic field); (c) common (1–4 in the microscopic field); (r) rare (a few specimens in the preparation field series); (f) few (a few specimens in the preparation).

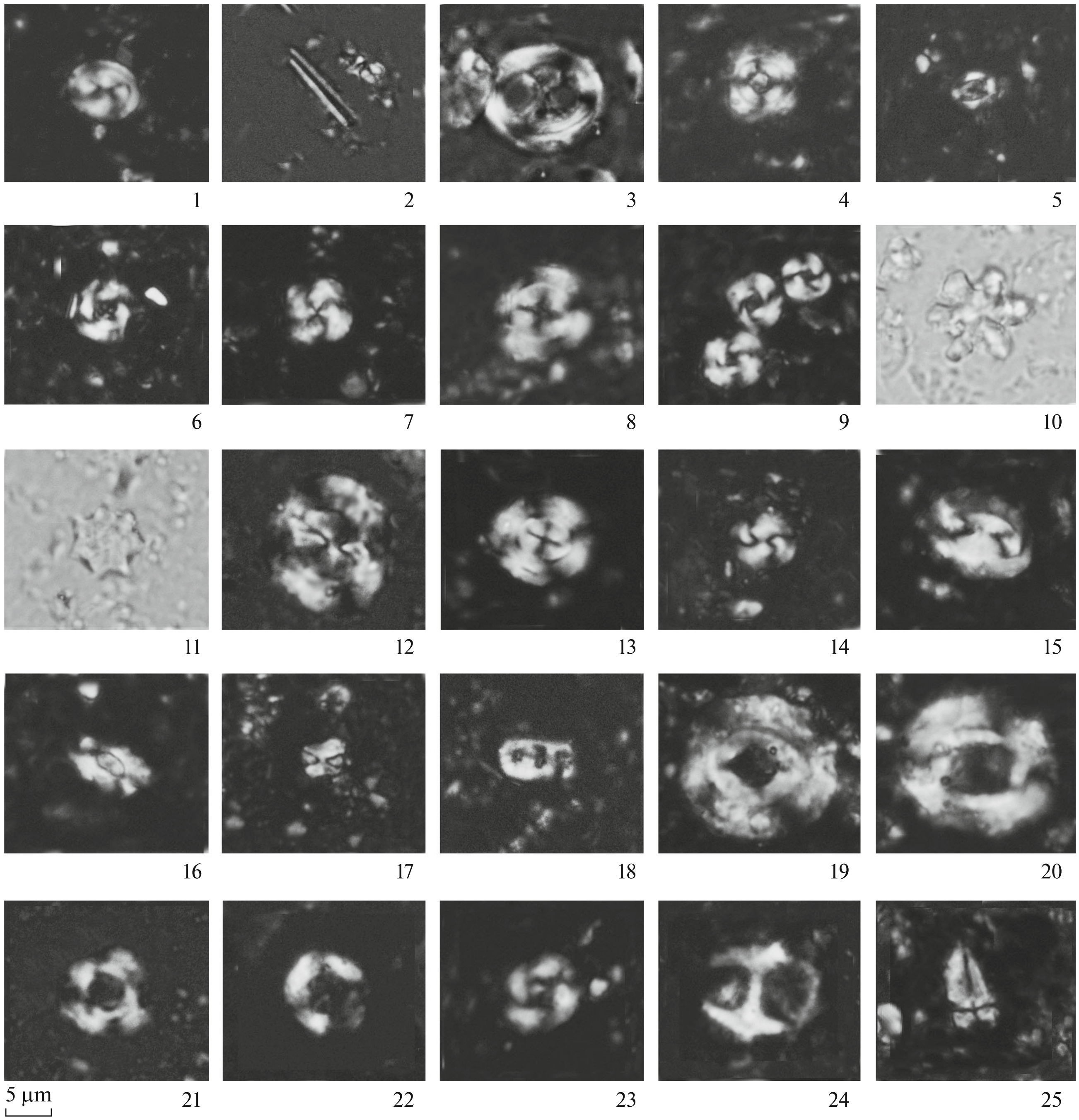

Fig. 3. Photomicrographs of the calcareous nannoplankton in the Upper Eocene–Lower Oligocene interval of the Chirkei section. All images except 10 and 11 were taken under crossed nicols. (1) *Bicolumnus ovatus* Wei and Wise, sample 211; (2) *Blackites spinosus* (Deflandre and Fert) Hay and Towe, sample 219; (3) *Chiasmolithus oamaruensis* (Deflandre) Hay, Mohler and Wade, sample 219; (4) *Coccolithus formosus* (Kamptner) Wise, sample 203; (5) *Clausicoccus subdistichus* (Roth) Prins, sample 510; (6) *Cribrocentrum reticulatum* (Gartner and Smith) Perch-Nielsen, sample 214; (7) *C. erbae* Fornaciari, Agnini, Catanzariti, Rio, Bolla, Valvasoni, sample 204; (8) *C. isabellae* Fornaciari, Agnini, Catanzariti, Rio, Bolla, Valvasoni, sample 207; (9) *Cyclicargolithus floridanus* (Roth and Hay) Bukry, sample 210; (10) *Discoaster nodifer*, sample 510; (11) *D. saipanensis* Bramlette and Riedel, sample 207; (12, 13) *Dictyococcites bisectus*: (12) sample 217, (13) sample 210; (14) *D. scrippsae* Bukry and Percival, sample 215; (15) *Helicosphaera compacta* Bramlette and Wilcoxon, sample 218; (16) *Helicosphaera* sp. 3 sensu Bown, 2005; (17) *Lanternitus minutus* Stradner, sample 203; (18) *Isthmolithus recurvus* Deflandre in Deflandre and Fert, sample 214; (19) *Reticulofenestra hillae* Bukry and Percival, sample 510; (20) *R. umbilicus* (Levin) Martini and Ritzkowski, sample510; (21) *R. circus* de Kaenel and Villa, sample 467; (22, 23) *R. ornata* Müller: (22) sample 552, (23) sample 553b; (24) *Pontosphaera fibula* Gheta, sample 552; (25) *S. pseudoradians* Bramlette & Wilcoxon, sample 211.

face in its modern understanding based on the disappearance of foraminifers Hantkeninidae (Vandenberghe et al., 2012), corresponds to the base of zone CNO0. Termination of the bloom of this species corresponds to the base of subzone CP16b. Thus, the Eocene/Oligocene interface likely occurs in the uppermost part of the Belaya Glina Formation.

The last occurrence of *Coccolithus formosus*, which is the common marker for all three scales, records the base of zones NP22, CP16, and CN1 (Table 1, Fig. 3). This event is established approximately 34 m above the base of the Pshekh Subformation (sample 470) immediately above the limestone interlayer. The last occurrence of *Reticulofenesra umbilicus*, which records the base of zones NP23, CP22, and CNE2, is defined approximately 14 m upward the section (sample 462). This level is underlain by noncarbonate clays of upper units of the Pshekh Formation. Therefore, the last occurrence of *R. umbilicus* and, correspondingly, the base of zones under consideration, cannot reliably be determined.

The Ostracoda bed in the lower part of the Solenov Formation includes an extremely poor nannoplankton assemblage, which is characterized by the presence of rare specimens of the endemic species of Paratethys (*Reticulofenestra ornata* and *Pontosphaera fibula*) that are widespread in the organic-poor sections (Báldi-Beke, 1981; Krhovsky et al., 1992; Melinte-Dobrinescu and Brustur, 2008; Nagymarosy and Voronina, 1992; Roban and Melinte, 2005; Sachsenhofer et al., 2017) and, probably, are adapted to salinity fluctuations in the basin (Melinte, 2005). This is the recorded uppermost nannoplankton level in the Chirkei section.

LITHOLOGY OF UPPER EOCENE AND LOWER OLIGOCENE ROCKS

Belaya Glina Formation. Rocks of this formation (thickness about 40 m) are represented by an alternation of pale gray limestone and marl beds (Figs. 4, 5). The $CaCO_3$ content in rocks varies from 20 to 80%. The marl/limestone intercalation makes up the smallest (decimeter-scale) cyclothemes. Such beds are grouped into sedimentary cycles of a larger order (1.5–2.5 m thick) dominated by marls and limestones in the lower and upper part, respectively (Figs. 5a–d). Rocks of this formation show numerous traces of bioturbation with the width varying from a few millimeters to 1 cm (*Rhizocorallium* and others, Figs. 5e, 5f) and they lack traces of active currents (flows). The complex of lithological, geochemical, and paleontological properties suggests that sedimentation in the Belaya Glina epoch took place in a normally aerated large basin with a relatively sluggish hydrodynamics (at least, below the wave agitation zone). The top of the Belaya Glina Formation includes the limestone/marl intercalation bed overlain by the Maikopian dark (mainly clayey) rocks with a sharp boundary (Figs. 5b, 5c).

The microscopic examination of thin sections shows that rocks of the Belaya Glina Formation lack microlamination, but they include flattened ellipsoid patches (tracks of ichnofaunas) and numerous inclusions of foraminiferal tests.

The carbonate material is the major component in rocks of this formation. Based on the XRF data, the carbonate material is represented mainly by calcite, with a notable variation in different parts of the Upper Eocene sequence: from 37% in marl beds to 60–85% in limestone beds. As is evident from Fig. 4, the highest variations in the carbonate material content are typical of the lower half of the formation. The content is slightly lesser (40–60%) upward the section and again higher (up to 80–85%) toward the top of the sequence.

Khadum Formation. This unit includes the Pshekh and Solenov subformations. It is mainly composed of dark gray (almost black and carbonate-rich at some intervals) mudstones that differ sharply from the Belaya Glina rocks (Fig. 6a).

Pshekh Subformation. The lower part of this sequence includes several thick (~0.15–0.25 m) interlayers of fine-grained sandstones (Fig. 6b), with thickness along the strike varying considerably up to the point of pinchout. Their formation at the initial stage of paleobasin evolution was triggered by the drastic activation of basin hydrodynamics and the input of sandy material.

The clayey rocks lack large traces of the vital activity of benthic organisms similar to those in the Belaya Glina section. Relicts of shells are also missing. They show a small-scale cyclicity composed of an intercalation of layers (0.1–0.2 m) of foliated (thin platy) mudstones and clayey rocks represented by relatively thick platy and more massive mudstones. The foliated and thick platy mudstones lie in the lower and upper part of the cyclothemes, respectively (Fig. 6c). On the whole, the sequence shows a relatively monotonous structure.

The Belaya Glina-to-Pshekh sequence transition is marked by a decrease of the carbonate content from 60–70 to *n*% in the lower part (6–7 m) and its increase up to 30–40% in the middle part of the Pshekh sequence. However, the carbonate content decreases gradually upward the section and the Pshekh sequence is composed of noncarbonate rocks in the upper part. Analogous noncarbonate rock interval is also recorded at this level in other areas of the Northern Caucasus (Somov, 1965). As in the Belaya Glina Subformation, the carbonate material in this sequence is mainly represented by calcite. However, the content of dolomite in the limestone bed located 15 m above the Pshekh sequence base (Fig. 4, sample 531) is comparable with that of calcite. Some samples from this sequence also contain the dolomite admixture (diffractograms show reflections with slightly elevated $d/n \sim 2.903$ Å).

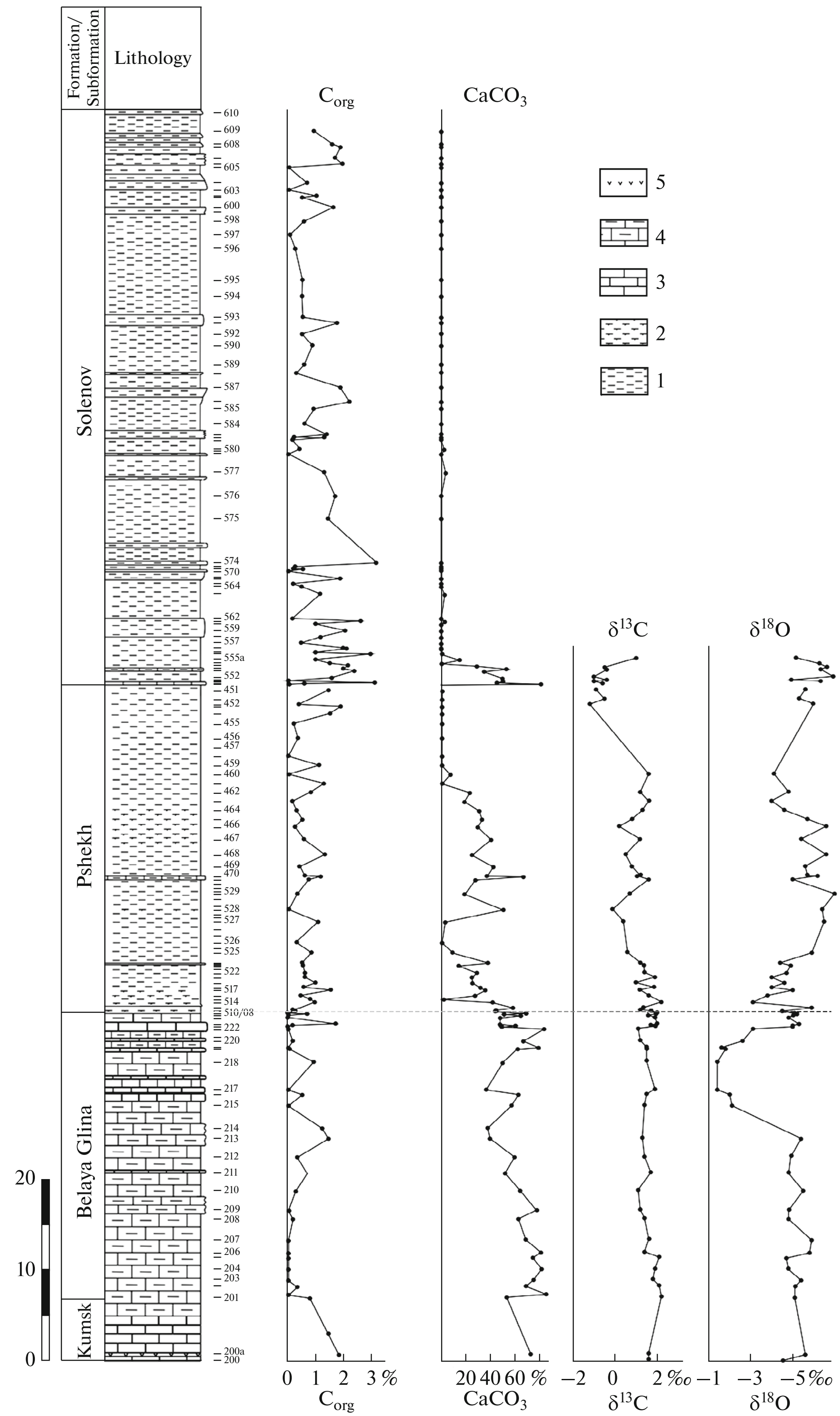

Fig. 4. Lithological structure of the Belaya Glina and Khadum formations and distribution of C_{org}, $CaCO_3$, $\delta^{13}C$, and $\delta^{18}O$. (1) Clayey rocks, (2) clayey–marly rocks, (3) limestone, (4) clayey limestone, (5) bentonite interlayers.

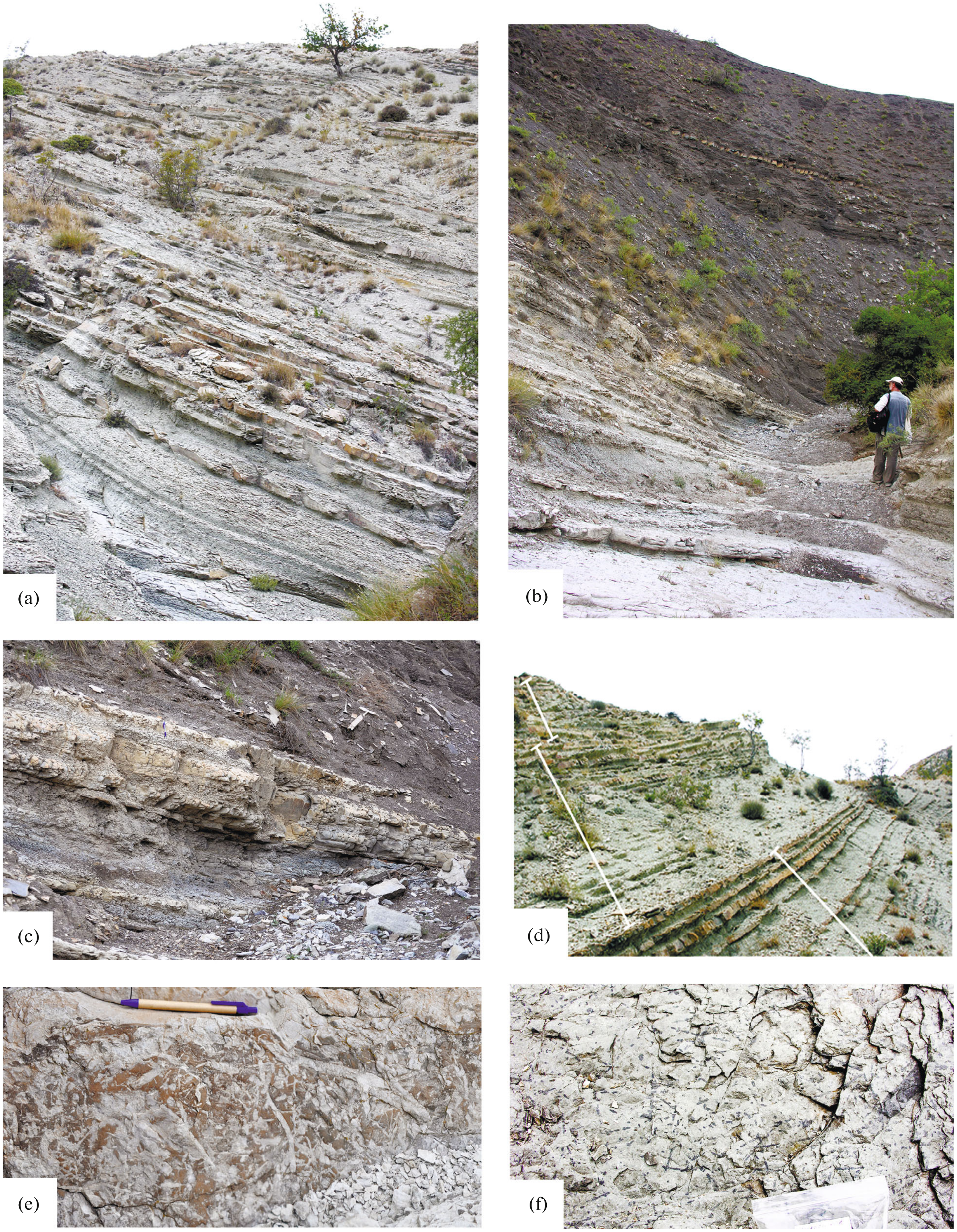

Fig. 5. Rocks of the Belaya Glina Formation. (a) Intercalation of limestone and marl layers in the formation; (b) upper horizons of the Belaya Glina Formation and overlying rocks of the Pshekh Subformation; (c) contact of pale limestones at the top of the Belaya Glina Formation and dark mudstones at the base of the Pshekh Subformation; (d) sedimentation cycles of the Belaya Glina Formation (up to a few meters thick); (e, f) traces of the vital activity of diverse ichnofauna in rocks of the Belaya Glina basin , (c) ceclites in the upper part of the subformation.

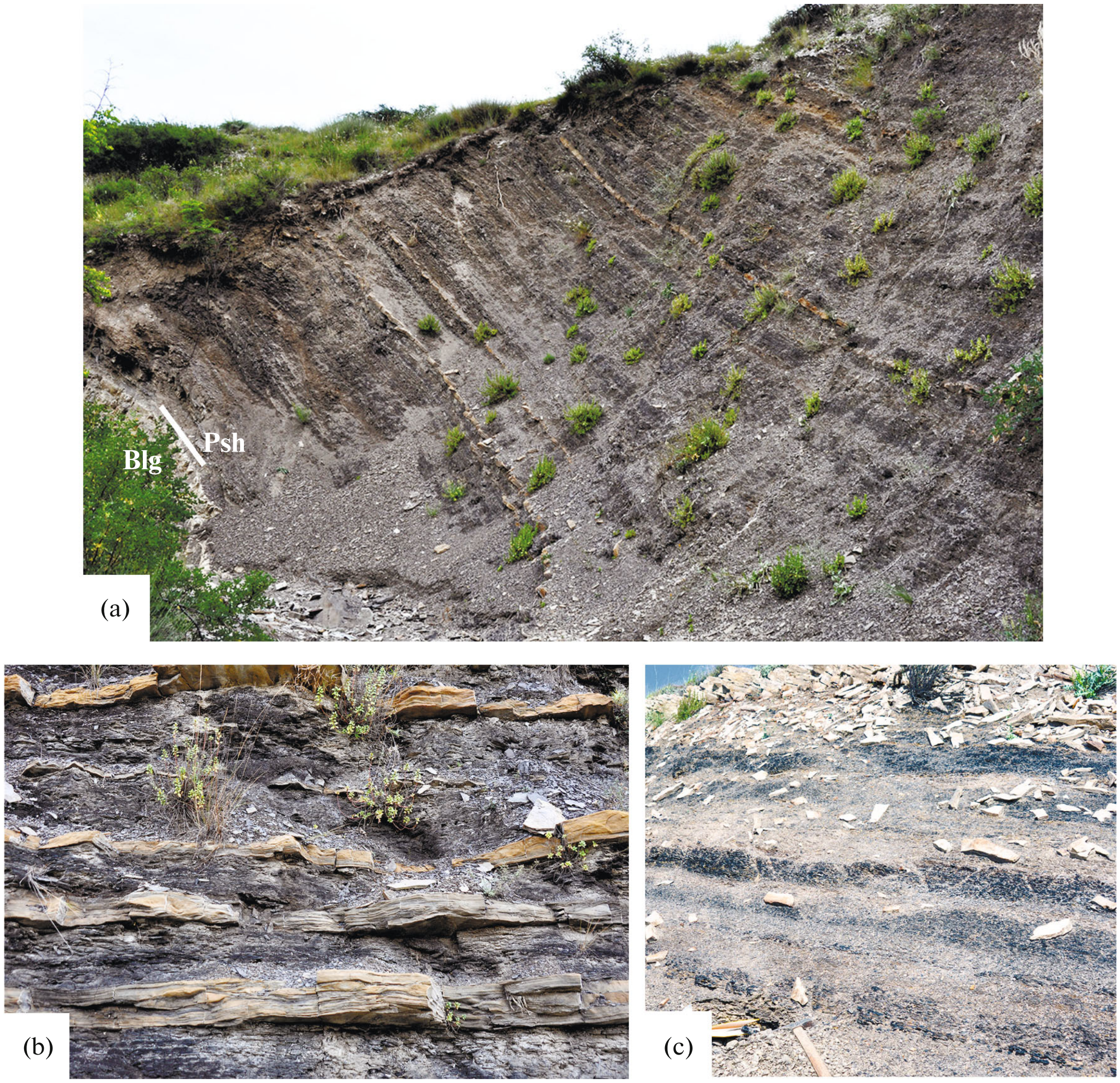

Fig. 6. Rocks of the Pshekh Subformation. (a) Rocks in the lower part of the Pshekh Subformation (Psh), contact with rocks of the Belaya Glina Formation (Blg) is shown in the left, (b) fine-grained sandstone member 3 m above the sequence base, (c) ceclites in the upper part of the subformation.

Issue of the sulfide mineralization in rocks of the Khadum Formation is of particular interest. Although the content of Fe, S and C_{org} in clayey rocks is sufficiently high, the rocks lack relatively large (millimeter- to centimeter-scale) sulfide concretions. At the same time, the study of rocks with optical and electron microscopic microscopes revealed a large amount of the authigenic framboidal pyrite with diverse morphology (Fig. 7). The pyrite is mainly observed as rounded framboids composed of numerous small and well-faceted pyrite crystallites. Framboids in the clayey rocks can be grouped into framboidal aggregates.

Solenov Subformation. The base of this subformation includes the Ostracoda Horizon, which comprises a limestone bed 0.35–0.4 m thick (Figs. 8a, 8c) and carbonate–clayey rock layers (~1.5 m thick). The limestone bed has a sharp contact with the underlying rocks. The top of the bed is marked by distinct and large ichnofauna traces similar to those in the Belaya Glina rocks. Thin sections of clayey rocks from this horizon show Ostracoda shells.

Rocks overlying the Ostracoda Horizon have a different appearance: almost complete lack of the carbonate admixture; appearance of horizons (up to 1.5 m thick) dominated by thick platy mudstones that make up terraces on the slope (Figs. 8a, 8b, 8d). At the same time, these thick platy mudstone horizons comprise several (up to 10) small cyclothemes of the type described above but with a lesser thickness (Fig. 8e). The topmost part of the section (Fig. 8b) is marked by the thinning and decrease of these horizons up to the

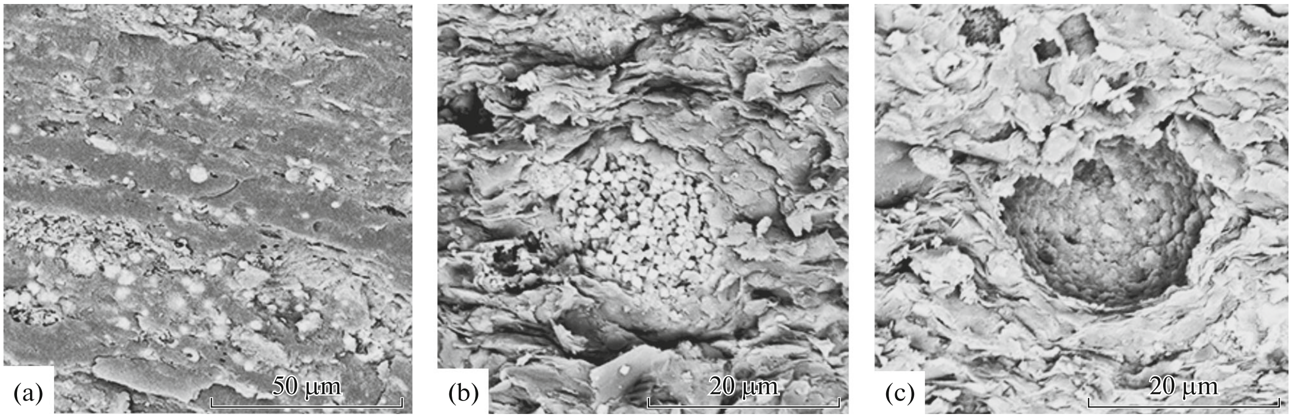

Fig. 7. Photomicrographs of pyrite framboids in rocks of the Pshekh Subformation. (a) Clayey rock with abundant framboid inclusions; (b, c) framboids.

point of their disappearance and their replacement by sandy interlayers (10–20 cm). Here, the sandstone interlayers make up several cyclothemes each up to 3 m thick. They likely correspond to the Miatly sandstone sequence, which distinctly overlies the Khadum sequence in the northern section exposed along the Sulak River. The overlying part of the section includes a thick unit with large olistoliths of the pre-Maikopian rocks.

Intercalation of the thin and thick platy mudstones in the section produces a relatively coarse cyclicity, with the thin platy and thick platy varieties dominating in the lower and upper parts, respectively, of the cyclothemes up to a few meters thick (Figs. 8a–8e). Despite these discrepancies, the Solenov mudstones are similar to clayey of the rocks Pshekh Horizon (thin bedding, lack of benthic fauna, and so on). In addition, rocks of both Belaya Glina Formation and Solenov Subformation are characterized by similar structures of sedimentary cyclothemes therein.

The Solenov Subformation includes several horizons with the distorted primary sedimentary rock structure (folding, mixing, jointing, local angular unconformities, and others) related to paleoseismic events in the region (Gavrilov, 2016, 2017).

Organic Matter Content in Rocks of the Belaya Glina and Khadum Formations

Distribution of organic matter (OM) is appreciably irregular in Eocene–Oligocene sedimentary assemblages of the northeastern Caucasus. For example, the C_{org} content is as much as 2 to 3% in rocks of the Bartonian Kumsk Formation, but almost negligible in rocks of the Belaya Glina Formation and, particularly, in its lower part (Fig. 4). In the upper part of the sequence, the C_{org} content is slightly higher (usually 0.*n*%) and as much as 1.27 and 1.48% only in two samples from the middle part of the sequence.

Transition to rocks of the Pshekh Subformation is accompanied by a more regular distribution of C_{org}, which varies from 0.5 to 1.5% and reaches 2% in some samples.

In the Solenov Subformation, the Corg content increases to 2–2.5% in rocks overlying the Ostracoda bed at an interval of 4–5 m. On the whole, despite a relatively irregular distribution of C_{org} in rocks, as compared to rocks of the Pshekh sequence, this part of the section includes much more intervals with the C_{org} content reaching 2.5% or more.

Petrographic study of the Khadum sequence indicates a universal presence of OM therein. All types (clayey–carbonate, clayey, silty–clayey) of studied sediment are dominated by the amorphous OM (AOM, colloalginite) with different tints of the brown color. The subordinate coalified terrestrial plant detritus, which is characterized by the fine (silt) dimension, generally accounts for a small fraction of total OM. We should also mention a relative scarcity of the terrestrial palynomorphic components. Morphology of the AOM particles is controlled mainly by the textural-structural features of sediments, which, in turn, depend upon the proportion of major sedimentary components and upon the degree of the sediment bioturbation.

So, the more ore less homogeneous matrix of limestones and marls, which are mainly composed of the calcareous nannoplankton remains, usually contains a relatively homogeneous finely dispersed and uniformly distributed amorphous OM. But the patchy AOM distribution is more typical for the bioturbated carbonate–clayey and silty–clayey sediments. In rocks of the Khadum Horizon with the highest clay content, i.e., fissile mudstones, which commonly show a prominent lamination and only slightly disturbed by small burrows (Chondrites), AOM usually occurs as tiny (0.05–0.2 mm) flattened lenticles oriented along the bedding or as numerous fine

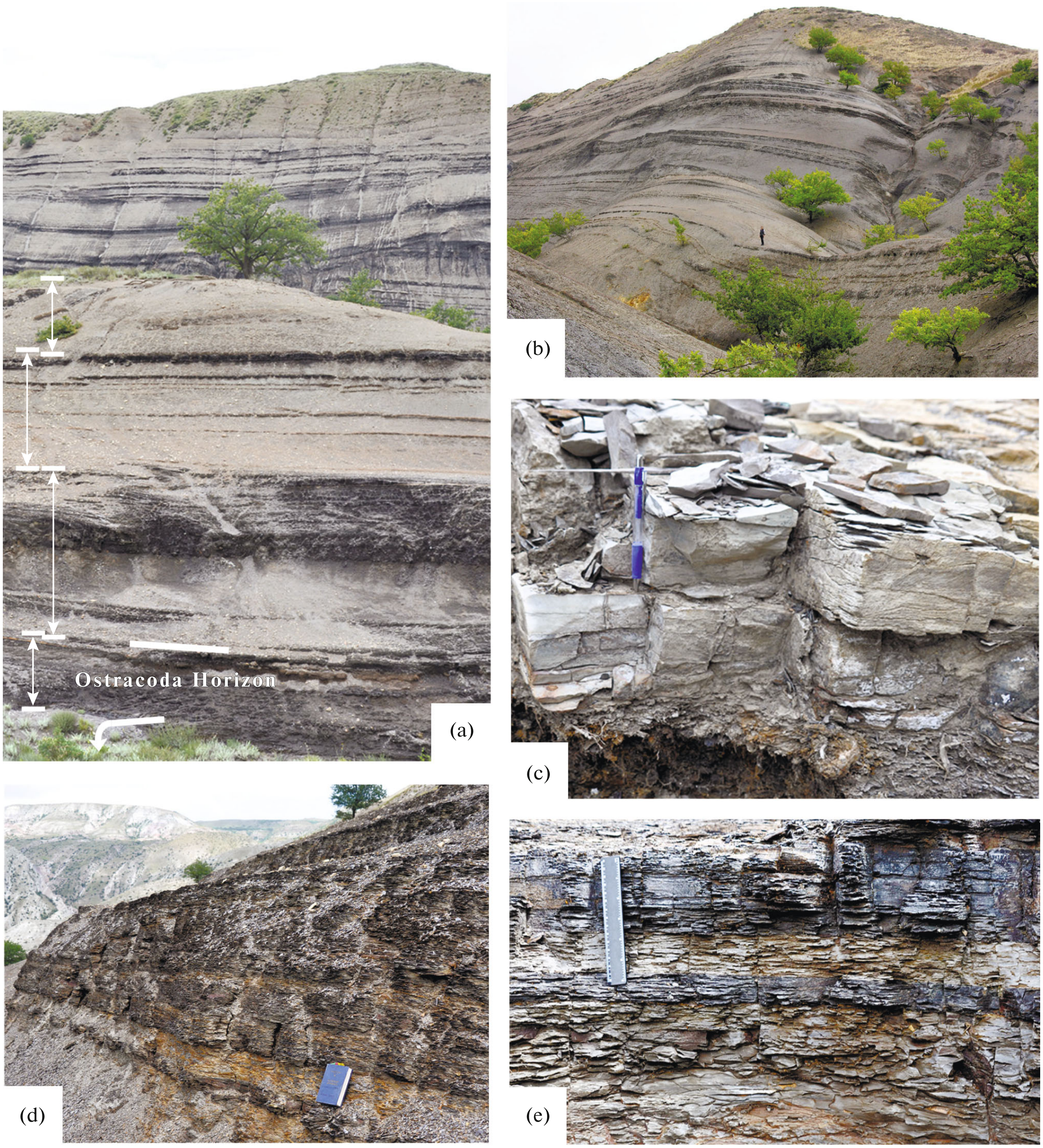

Fig. 8. Rocks of the Solenov Subformation. (a) Lower part of the Solenov Subformation showing the sedimentation cyclicity (fancy arrow shows the position of limestone bed in Ostracoda Horizon, (b) upper part of the Solenov subformation, (c) structure of the limestone bed, (d–e) horizon of thick platy mudstone with cyclic structure.

(0.01–0.02 mm) discontinuous laminas that are often impregnated with the framboidal pyrite.

As a typical, the dark reddish-brown organic inclusions, resembling the freshwater algae (Prasinophytes) in their morphology, but subjected to strong catagenetic processing, are scattered within some intervals of the Pshekh Subformation.

Rock Eval Parameters in Rocks of the Khadum Formation

Pyrolitic parameters of the studied Khadum rocks (31 samples) are presented in Table 2. The total organic carbon content (TOC) detected by the Rock Eval pyrolysis varies from 0.36 to 2.85%. An increased TOC content (>1%) is typical for the majority of the studied (23) samples. The highest TOC contents (>2%) are recorded over the section more or less regularly in the clayey and carbonate–clayey rocks that usually contain a very small silty admixture (<10%). The low TOC content (<1%) is recorded usually in rocks with a high content of the terrigenous silty material as well as in some intensely bioturbated clayey and carbonate–clayey rocks.

Values of the hydrocarbon (HC) generation potential (Table 2) characterize the major part of Khadum rocks in the Chirkei section (21 samples) as oil source rocks with the HC generation potential ranging from the moderate (2–6 mg HC/g) to high (>6 mg HC/g) category. Low values of the HC potential (<2 mg HC/g) are recorded in the clayey–silty (intensely bioturbated in some places) rock interlayers.

Temperature of hydrocarbon yield was measured by the thermal breakdown of samples. In most cases (30 samples), the maximum temperature of hydrocarbon yield (T_{max} = 433–452°C) exceeds the boundary value T_{max} = 430°C, which defines the initial stage of OM maturity (Table 1, Fig. 9). This fact suggests that rocks of the Khadum Formation contain mainly mature kerogen, which underwent the catagenetic transformation and reached the main zone of oil formation. Values of the productivity coefficient or production index (PI) determined for rocks of the Khadum Horizon (0.09–0.55) and respective values of their bituminosity (Table 2) define an interval (0.1–0.4), which is typical of oil generation zones (Tisso and Welte, 1978).

Values of the hydrogen index (HI) in rocks of the Khadum Formation is currently characterized by low values (52–351 g HC/g TOC). The oxygen index (OI) values, in general, are fairly low and in the majority of studied samples, correspond to the catagenetically transformed OM. Based on the HI/OI ratio (Fig. 10), these rocks can be assigned to the variety mainly containing the marine kerogen (type II, Table 2, Fig. 10). The majority of studied samples is classified as containing type III kerogen, genetically related to the terrestrial plant or marine OM but significantly transformed by processes of oxidative decomposition.

To interpret correctly the origin of kerogen in sediments of the Khadum succession, we should take its relatively high maturity into consideration. This approach suggests the loss of a significant portion of hydrocarbons during catagenetic processes and maturation of kerogen. These processes were likely accompanied by a decrease of HI values. Thus, the initial HI values for the kerogen in Khadum rocks, which were

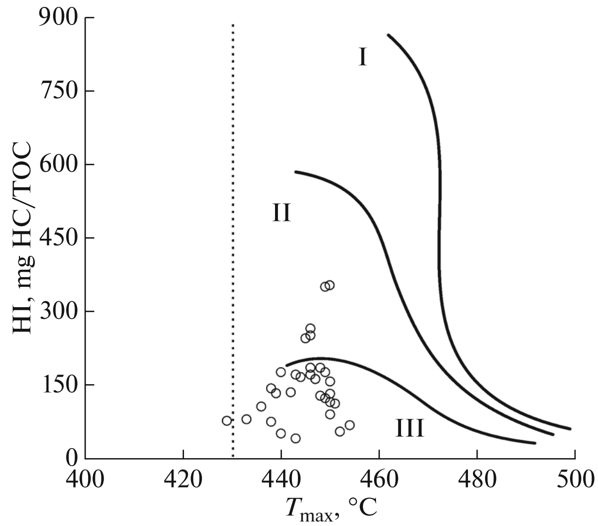

Fig. 9. Plot of hydrogen index (HI) versus temperature of maximum hydrocarbon (HC) yield (T_{max}) for rocks of the Khadum Formation in the Chirkei section. Dots show T_{max} = 430°C determining the kerogen maturity (Tissot and Welte, 1978).

not subjected to catagenetic transformations, could also be higher. Probably, such values more completely reflected the genetic (aquagenic?) origin of OM in rocks. This assumption is in agreement with the petrographic observations indicating a low content of the terrestrial organic components, but significant amount of the amorphous OM, and presence of the algal (hydrocarbon-rich leiptinite) components in the OM of the Khadum Formation. However, one cannot also rule out the transport of a dissolved terrestrial organic (humic) matter into distal zones of marine sedimentation, and its subsequent involvement in the formation of kerogen.

Carbon and Oxygen Isotopes in the Chirkei Section

The behavior of carbon and oxygen isotopes in Upper Eocene and Lower Oligocene rocks is of great interest, because these rocks were accumulated in significantly different geochemical settings. Moreover, the Eocene/Oligocene boundary was marked by global climate changes, which affected the behavior of isotopes in rocks in other areas of the Earth.

To assess the behavior of $\delta^{13}C$ and $\delta^{18}O$ in rocks of the Chirkei section, we analyzed 66 samples containing the carbonate material. Noncarbonate rocks of the Solenov sequence overlying the Ostracoda Horizon were not analyzed.

The total scatter of isotope values in carbonates from the Belaya Glina and Khadum sequences is as follows: $\delta^{13}O$ from –0.9 to 2.2‰ PDB and $\delta^{18}O$ from –6.9 to 1.4‰ PDB (Table 3). The carbon isotopic composition in the main group is rather homogeneous

Table 2. Pyrolitic parameters of rocks in the Khadum Formation (Chirkei section)

Ord. no.	Sample	S_1	S_2	$S_1 + S_2$	PI	T_{max}	TOC	HI	OI
		free HC in the rock (recovered at <300°C), mg HC/g	HC products of the kerogen and resinous-asphaltene matter (recovered at 300–600°C), mg HC/g	generation potential	$S_1/(S_1 + S_2)$ productivity index, bituminosity degree	temperature of maximum HC yield at pyrolysis of kerogen, °C	total content of organic carbon in rock, wt %	hydrogen index, mg HC/g TOC	oxygen index, mg CO_2/g TOC
		Solenov subformation							
1	564	0.22	0.37	0.59	0.37	440	0.71	52	15
2	563	0.58	3.77	4.35	0.13	449	2.13	177	2
3	562	0.31	0.66	0.97	0.32	450	0.57	116	28
4	560	0.38	1.21	1.59	0.24	429	1.56	78	19
5	558/2	0.39	1.36	1.75	0.22	433	1.68	81	11
6	558/1	0.49	1.79	2.28	0.21	436	1.68	107	9
7	557	0.63	0.59	1.22	0.52	438	0.78	76	6
8	556c-2	0.99	3.74	4.73	0.21	438	2.59	144	7
9	556c	0.29	2.98	3.27	0.09	439	2.22	134	7
10	556a	0.45	2.67	3.12	0.14	442	1.96	136	4
11	554c	0.45	3.1	3.55	0.13	443	1.80	172	4
12	554a	1.38	7.76	9.14	0.15	449	2.21	351	10
13	552	1.39	6.21	7.60	0.18	449	1.81	343	15
14	450	0.97	7.58	8.55	0.11	446	2.85	266	19
		Pshekh subformation							
15	549	0.19	0.15	0.34	0.55	443	0.36	42	25
16	453	0.63	5.47	6.10	0.1	446	2.17	252	17
17	459	0.82	4.78	5.60	0.15	445	1.94	246	20
18	461	0.39	2.53	2.92	0.13	440	1.43	177	45
19	466	0.08	0.28	0.36	0.21	452	0.50	56	252
20	468	0.64	2.38	3.02	0.21	448	1.28	186	88
21	530	0.87	1.55	2.42	0.36	450	0.98	158	34
22	529	1.31	4.30	5.61	0.23	446	2.31	186	15
23	527	0.88	2.44	3.32	0.26	447	1.50	163	11
24	525	1.11	2.32	3.43	0.32	446	1.35	172	23
25	523	0.53	0.71	1.24	0.43	448	0.55	129	33
26	522	0.72	1.22	1.94	0.37	444	0.73	167	26
27	519	0.31	2.82	3.13	0.10	449	2.28	124	54
28	518	0.05	0.54	0.59	0.09	454	0.78	69	118
29	517	0.26	1.70	1.96	0.13	450	1.28	133	41
30	516t	0.29	2.04	2.33	0.13	451	1.80	113	58
31	514	0.25	2.21	2.46	0.1	450	2.42	91	78

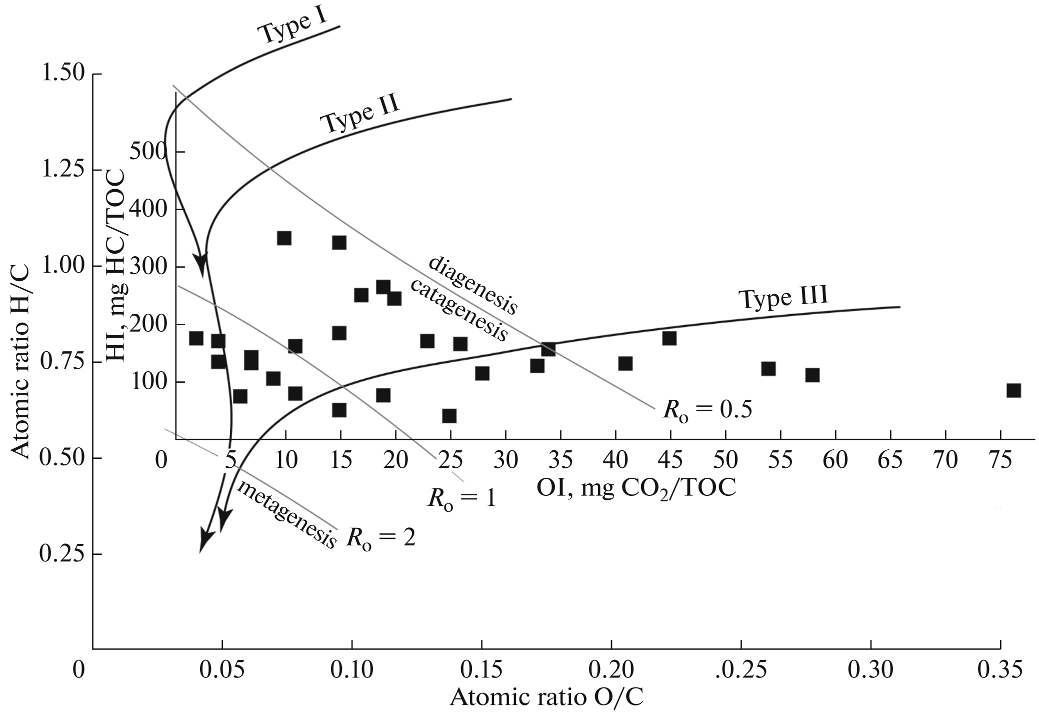

Fig. 10. Classification of kerogen and determination of the OC transformation degree in rocks of the Khadum Formation on the plot of hydrogen (HI) vs. oxygen (OI) indexes corresponding to atom ratios H/C vs. O/C in different types of kerogen kerogens on the modified Van Krevelen diagram (Tissot and Welte, 1978; Tyson, 1995). (R_o) Coefficient of vitrinite reflectance (arrows show directions of the structural evolution of kerogen with increasing depth of rock submergence.

and falls into the interval of 1 to 2‰ except in rare cases. Variations in the oxygen isotopic composition are more significant and evidently related to certain stratigraphic intervals.

The oxygen isotope curve is marked by a drastic increase of $\delta^{18}O$ in the upper part of the Belaya Glina Formation (10–12 m below its top). In the lower part of the sequence, the average $\delta^{18}O$ value is -5.2 ± 0.4‰. In the upper part, the value is more than 3‰ higher (up to 2.0 ± 0.6‰), but the carbon isotopic composition remains virtually unchanged. Taking into consideration the relatively homogeneous lithology of the Belaya Glina rocks, which are appreciably enriched in $CaCO_3$ (40–60% or more), the isotopic anomaly can be attributed to a drastic cooling about 34 Ma ago (total effect of the decrease of water temperature and ^{18}O in the ocean due to the appearance of ice sheet on Antarctica).

Average $\delta^{18}O$ and $\delta^{13}C$ values in carbonates from the Pshekh sequence are close to those in the lower part of the Belaya Glina Formation. However, these parameters show linear correlation in the Pshekh sequence (Fig. 11), probably, related either to periodic variation of water salinity in the basin or to irregular postsedimentary changes in rocks. In either case, maximum $\delta^{18}O$ values should be considered the best proxies for paleoclimatic reconstructions: these values are higher in rocks from the lower part of the Belaya Glina Formation, but lower than in the upper part. Let us note that the lower and upper parts of the Pshekh Horizon lack any distinction in the $\delta^{18}O$–$\delta^{13}C$ plots and show a virtually identical trend with similar values of the correlation coefficient.

Chemical Elements in Rocks of the Chirkei Section

To assess the behavior of chemical elements in lithologically and chemically different rocks in 130 samples from the Chirkei section, we determined a wide range of elements: Al, Si, Fe, Mn, P, S, Ti, V, Cr, Ni, Co, Zn, Pb, Cu, Ga, Rb, Sr, Ba, As, Th, U, and Mo. Table 4 presents average contents of these elements in stratigraphically and lithologically different sequences. Analysis of the distribution of elements in different sequences shows that variations of their concentration along the section are regular, but their orientation is not similar. Upward the section from the carbonate-dominated rocks of the Belaya Glina Formation to terrigenous rocks of the Khadum Formation, elements of the major group demonstrate about 2 to 4 times increase of concentrations that generally exceed average values of the respective elements (clarke values) calculated for the specified rock type (Turekian and Wedepohl, 1961; Vinogradov, 1962). As is evident form Table 4, this group also includes elements marked by much higher concentrations, e.g., As and

Table 3. Carbonate content in rocks, C_{org} content, and C and O isotopec compositions in carbonates from Upper Eocene and Lower Oligocene rocks in the Chirkei section

Sample	C_{org}, %	Carbonate content, %	$\delta^{13}C$, ‰ PDB	$\delta^{18}C$, ‰ PDB
Solenov Subformation				
555a	1.04	14.89	1	–4.85
554a	2.23	29.33	–0.1	–6.2
553b	2.02	54.58	–0.5	–6
553a	2.39	34.45	–0.3	–5.9
552	1.58	50.14	–1.0	–6.5
551	<0.1	50.37	–0.5	–4.8
550	5.1	46.28	–0.8	–6.0
550a	0.63	82.55	–0.5	–5.0
Pshekh Subformation				
460	<0.1	7.62	1.6	–4.0
462	0.83	23.54	1.2	–4.0
463	0.2	18.99	1.7	–3.6
464	0.36	30.93	1.3	–4.5
465	0.56	33.43	0.8	–5.5
466	0.29	29.86	0.5	–6.0
467	0.62	40.82	1.2	–5.4
468	1.36	25.24	0.6	–6.0
469	0.48	42.64	0.9	–5.3
470	0.64	37.63	1.5	–5.2
531	1.21	67.31	1.5	–5.6
530	0.78	27.97	1.6	–5.0
529	0.38	19.44	0.8	–6.9
528	?	50.37	0	–6.4
527	1.12	4.43	?	–6.5
525	0.88	9.78	0.7	–6.1
524	0.55	39.23	1.3	–4.4
523	0.58	14.33	1.4	–4.55
522	0.65	29.22	1.5	–4.7
520	0.64	25.81	1.9	–4.0
519	1.03	26.15	1	–4.6
518	0.60	32.06	1.8	–4.0
517	1.57	36.73	1.2	–5
516	0.52	27.63	1.6	–3.8
514	1.00	42.52	2.2	–3.1
513	0.51	26.00	1.4	–5.9
512	0.23	48.78	1.2	–5.0
511	0.32	44.23	1.7	–4.5
Belaya Glina Formation				
510	<0.1	62.31	1.4	–4.7
521c2	<0.1	68.79	2.1	–4.8
521c1	0.7	51.85	1.9	–5.1
521b-2	<0.1	88.00	1.6	–5.0
521b-1	<0.1	48.32	2	–4.6
521a	1.74	48.01	2.1	–4.9
521d2	0.22	61.28	1.7	–4.9
521d1	<0.1	50.03	1.9	–4.9
222	<0.1	84.02	1.1	–3.1
220	0.22	67.08	1.2	–2.6
219a	0.1	61.97	1.5	–1.8
219	<0.1	79.48	1.5	–1.6
218	0.96	50.71	1.5	–1.4
217	<0.1	36.73	1.9	–1.4
216	0.55	63.10	1.5	–2.0
215	<0.1	57.30	1.4	–2.1
214	1.27	37.98	2	–4.9
213	1.48	39.80	1.3	–5.4
212	0.38	59.92	1.4	–4.9
211	0.73	52.19	1.7	–4.8
210	0.33	64.47	1.1	–5.5
209	<0.1	77.66	1.2	–4.8
208	0.23	63.10	1.4	–4.8
207	<0.1	69.13	1.6	–5.9
206	<0.1	81.41	1.4	–5.8
205	<0.1	74.81	2.1	–4.7
204	<0.1	81.98	1.9	–4.8
203	<0.1	75.38	1.8	–5.4
202	0.38	69.02	2.1	–5.1
201c	<0.1	85.84	2.2	–5.1

Mo (almost 25 times higher) and S (50 times). Analysis of sulfide framboids revealed that they often include Mo (1 to 2%), but molybdenum sulfides are lacking.

The subordinate group of elements, which are characterized by an opposite trend of concentration variation along the section, includes Mn and Sr. Relatively higher concentrations of these elements in rocks of the Belaya Glina Formation are likely related to their isomorphous presence in the calcite structure, which is the main rock-forming mineral in these rocks. Correspondingly, their concentrations are decreased in noncarbonate rocks of the Khadum Formation. It should be mentioned that very low Mn concentrations can also be caused by specific sedimentation settings due to oxygen deficiency in rocks and water column of the Khadum paleobasin.

Phosphorus, which does not enter any of these groups, is marked by weak variations in rocks of different age. Such behavior of P can likely be related to its redistribution in rocks during active processes of the reductive diagenesis.

Peculiarities of Late Eocene and Early Oligocene Sedimentation Basins

The lithological and geochemical data presented above suggest significantly different sedimentation environments in Late Eocene and Early Oligocene basins in the northeastern Caucasus. The presence of numerous and diverse traces of the activity of organisms (ichnofauna) in rocks of the Belaya Glina basin testifies to a quite favorable habitat environment and normal water aeration. Transition to rocks of the Khadum basin was accompanied by a drastic decrease in the species diversity of ichnofauna and even their complete disappearance at some intervals. In such cases, one can only see small (millimeter-scale) traces of burrowing organisms (Chondrites?) and some intervals of rather actively bioturbated sediments. These organisms were adapted both to the reductive setting in sediments of the Khadum basin and to the anoxic conditions in near-bottom waters.

Application of the qualitative (mainly, lithological and paleoecological) indicators of the hydrosulfuric contamination does not make it possible to define confidently local episodic variations in the gas regime in the near-bottom water and to decipher precisely levels of the appearance or disappearance of anoxic conditions in specified sections. The presence or absence of hydrosulfuric contamination in a basin during sedimentation can quantitatively be assessed by concentrations of some chemical elements that are highly sensitive to gas regime variations in the near-bottom water. For example, R.O. Hallberg (1974) proposed to use the (Mo + Cu)/Zn ratio as the stagnation coefficient. In works of E.M. Emel'yanov (1977, 1981), ratios of Mo, Cu, Se, Zn, and Mn concentrations were used as the criterion. However, contents of elements, such as Mo and Mn, in the sediment are most sensitive to gas regime variations in the near-bottom water. Therefore, geochemical reconstructions for Paleogene basins in our work are based on the stagnation coefficient proposed in (Kholodov and Nedumov, 1991).

Choice of precisely these elements was dictated by their diametrically opposite behavior in the oxic and anoxic environment. For example, Mo actively enters the sediment under conditions of the hydrosulfuric contamination. Its active precipitation is related to several reasons, coprecipitation with sulfides being the major one (Korolev, 1958). The oxic environment is favorable for the accumulation of Mo in the dissolved state. In contrast, Mn is intensively accumulated in the dissolved state in hydrosulfuric waters and it is deposited almost completely in the sediment as oxides in the case of oxic gas regime. Analysis of a large dataset on the Mo and Mn concentration in deposits of the present-day and ancient basins revealed that very low (thousandths of a unit) values of the stagnation coefficient testify the oxic sedimentation setting. Increase of the coefficient by hundredths or tenths of unit sufficiently confidently suggest an anoxic sedimentation setting. For illustrative purposes, Table 4 presents values of the stagnation coefficient multiplied by 100. In this case, values >1 indicate the existence of an anoxic environment in the paleobasin.

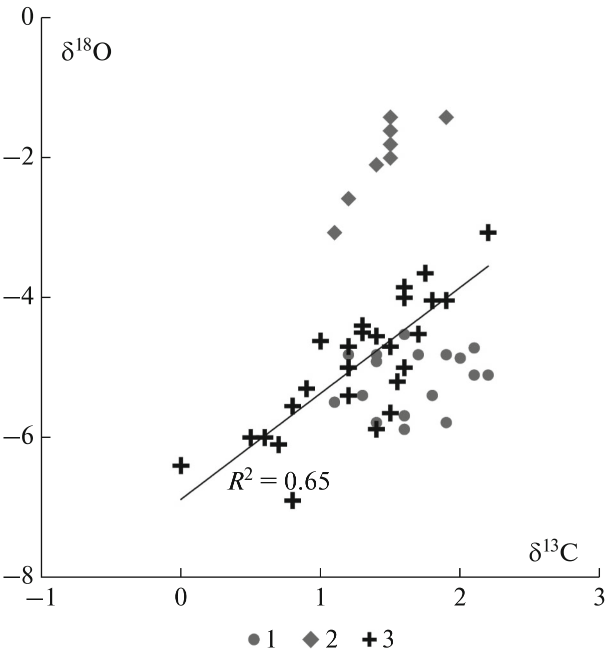

Fig. 11. Isotopic composition of carbon and oxygen in the Eocene/Oligocene transition sequences in the Chirkei section. (1) Bottom of the Belaya Glina Formation; (2) top of the Belaya Glina Formation; (3) Pshekh Subformation.

It should, however, be noted that the degree of anoxia in the Khadum basin could change gradually up to the point of its complete disappearance. First of all, this scenario is related to the onset of the Solenovian time marked by accumulation of sediments of the Ostracoda Horizon. As rocks of the Belaya Glina Formation, the Solenov limestone bed also shows large traces of fucoids. Stagnation coefficient here is estimated at 0.04 (limestone) and 0.23 (clayey marl). Thus, the results show that the geochemical setting in basin changed immediately after the Pshekhian time, and sediments of the Ostracoda Horizon were accumulated in actively aerated waters.

In addition, the main part of rocks of the Khadum Formation can demonstrate regular increase or decease of Mo concentrations at different levels of the sequence (Table 4). Such Mo variations also suggest possible periodic changes in the degree of anoxia in the paleobasin.

Enrichment of rocks with C_{org} promoted a high intensity of diagenetic processes in rocks of the

Table 4. Average contents of chemical elements and coefficients of their variation in rocks of the Chirkei section

	C_{org}	$CaCO_3$	Si	Al	Fe	Mn	Ti	P	S	V	Cr	Co	Ni	Cu	Zn	Pb	Ga	As	Rb	Sr	Mo	Ba	Th	U	Mo/Mn × 100
	%									10^{-4}%															
Belaya Glina Formation (21 samples)																									
Average content	0.34	65.18	10.48	4.28	1.75	0.25	0.19	0.04	0.018	67	33	9	39	44	43	29	7,8	1,1	42	1161	0.8	191	3.6	2.5	0.03
Standard deviation	0.43	15.12	3.85	1.37	0.77	0.05	0.08	0.02	0.039	24	13	5	13	32	15	7	1.9	0.5	16	168	0.0	19	1.4	0.6	0.005
Variation coefficient	128	23	37	32	44	19	40	42	218	36	39	57	33	73	35	23	24	40	39	14	0	10	39	23	17
Transitional member at top of the Belaya Glina Formation (8 samples)																									
Average content	0.36	59.73	15.82	4.93	1.90	0.26	0.32	0.08	0.22	78	51	13	50	53	51	18	9.4	11.9	59	935	3.5	189	4.4	1.0	0.17
Standard deviation	0.60	13.67	3.06	1.32	0.36	0.13	0.09	0.07	0.15	19	20	13	17	49	16	11	1.9	8.7	16	107	2.0	15	0.4	0.0	0.14
Variation coefficient	165	23	19	27	19	50	28	81	68	25	39	102	34	92	33	59	20	73	27	11	58	8	10	0	83
Maikop Group, Khadum Formation																									
Pshekh Subformation (38 samples)																									
Average content	0.68	23.63	26.64	8.13	2.98	0.05	0.49	0.06	0.42	184	108	13	62	74	92	27	14.7	19.4	111	448	25.3	356	9.0	5.9	7.3
Standard deviation	0.47	18.89	5.36	2.20	1.15	0.03	0.13	0.03	0.48	74	44	8	26	30	38	18	3.5	15.2	39	264	21.6	122	3.5	3.7	6.7
Variation coefficient	68	80	20	27	39	66	26	45	115	40	40	61	41	40	41	66	24	79	35	59	85	34	39	63	92
Solenov Subformation																									
Ostracoda Horizon, marl (2 samples)																									
Average content	2.87	64.30	8.53	1.66	2.30	0.55	0.08	0.06	0.24	32	2	1	32	20	25	8	4.4	1.4	13	1348	1.9	231	4.3	1.0	0.04
Ostracoda Horizon, clayey marl (5 samples)																									
Average content	1.65	43.70	22.64	7.52	2.03	0.18	0.44	0.09	0.43	119	83	10	96	99	101	25	13.2	13.4	79	778	4.0	272	6.1	1.3	0.23
Standard deviation	0.95	11.12	3.08	1.28	0.36	0.03	0.05	0.03	0.07	34	19	7	39	27	47	6	1.8	1.9	16	167	1.4	54	1.9	0.6	0.09
Variation coefficient	57	25	14	17	18	15	12	31	17	29	23	71	41	27	46	23	14	14	21	21	35	20	32	46	38
Solenov layers above the Ostracoda Horizon (86 samples)																									
Average content	0.97	0.67	31.09	10.84	4.08	0.05	0.57	0.05	1.06	188	121	30	98	147	145	49	20.9	25.8	140	151	23.4	688	12.4	7.9	15.5
Standard deviation	0.81	1.73	3.52	1.42	1.59	0.17	0.09	0.09	0.83	50	48	19	62	103	77	31	3.4	12.8	25	45	21.2	348	1.6	3.4	22.6
Variation coefficient	83	257	11	13	39	370	15	169	78	26	40	63	63	70	53	62	16	50	18	30	91	51	13	43	146

Khadum basin. First of all, this effect is reflected in the abundance of sulfides as pyrite framboids. Dolomite, a subordinate component in diffractograms of calcareous mudstones, is likely a diagenetic product. Processes of the reductive diagenesis were also responsible for the low contents of elements, such as Mn and P, in the rocks. During the evolution of the paleobasin under anoxic conditions, these elements could diffuse freely from the sediment to the near-bottom water and disperse therein. It is quite probable that processes of diagenesis affected the behavior of $\delta^{13}C$ and, particularly, $\delta^{18}O$.

Possible Reasons for the Catagenetic Transformation of Rocks in the Chirkei section

As noted above, the pyrolitic data on OM in rocks of the Chirkei testify to a high degree of its maturity. However, transformation of OM did not reach such maturation degree in other sections of the Maikop sequence. It is quite possible that the high maturity of OM in the Khadum rocks in the specified section is related to some local processes that intensified the catagenetic transformation of rocks. Since rocks of the Chirkei section did not subside to great depths relative to other sections, the geostatic load did not likely play a crucial role in the intensification of rock transformation. Intensification of these processes could be provoked by the presence of a pluton near this section at a relatively small depth, and the pluton could provide the appearance of local zones with strong heat flows. The high degree of OM transformation (maturation) could also be provoked by high paleoseismicity in this region of Dagestan (Gavrilov, 2016, 2017).

CONCLUSIONS

1. The results obtained indicate sharp lithogeochemical distinctions between the Upper Eocene and Lower Oligocene deposits in the northeastern Caucasus.

2. The nannoplankton data suggest that the Eocene/Oligocene interface in the Chirkei section occurs slightly below the Belaya Glina/Khadum boundary. The series of nannoplankton bioevents established in this section make it possible to accomplish its stratigraphic division based on three scales proposed by E. Martini (Martini, 1971), H. Okada and D. Bukry (Okada and Bukry, 1980), and K. Agnini with colleagues (Agnini et al., 2014) that are coded as NP, CP, and CNE/CNO, respectively.

3. Organic matter (OM) in rocks of the Khadum Formation in the Chirkei section is characterized by relatively high degree of maturity, which matches the main zone of oil formation. Initially, the rocks could be dominated by the marine OM with a terrigenous OM admixture.

4. Positive oxygen isotope anomaly in the upper part of the Belaya Glina Formation reflects obviously global climate changes (cooling) near the Eocene/Oligocene interface. Limitation of the anomaly by the upper boundary of the Belaya Glina Formation can be attributed to water salinity variations in the Early Oligocene basin and intense processes of early diagenesis of sediments.

5. The lithological, geochemical, and paleoecological data testify to oxygen deficiency in the Khadum paleobasin in the northeastern Caucasus. Such environment was unstable and periodically intensified or weakened. The paleoecological environment in the Belaya Glina basin was typical of normally aerated basins.

ACKNOWLEDGMENTS

The authors are grateful to the staff of analytical laboratories at the Geological Institute, Russian Academy of Sciences, for the analyses of sedimentary rocks.

This work was accomplished in accordance with the State Task of the Geological Institute, Russian Academy of Sciences (project nos. 0135-2016-0004, 0135-2014-0070, and 0135-2015-0031) and supported in part by the Russian Foundation for Basic Research (project no. 15-05-07556).

REFERENCES

Agnini C., Fornaciari E., Raffi I. et al. Biozonation and biochronology of Paleogene calcareous nannofossils from low and middle latitudes, *Newslett. Stratigr*, 2014, vol. 47, no. 2, pp. 131–181.

Akhmetiev, M.A., Gavrilov, Yu.O., and Zaporozhets, N.I., Events at the turn of the Eocene and Oligocene in the Central Eurasian region (middle latitudes), *Dokl. Earth Sci.*, 2017, vol. 473, no. 3, pp. 273–276.

Báldi-Beke, M., The nannoplankton of the Transdanubian Paleogene Formations, *Geol. Hungar. Ser. Paleont.*, 1981, vol. 43, pp. 1–307.

Bown, P.R. and Young, J.R., *Techniques*, in *Calcareous Nannofossil Biostratigraphy, Brit. Micropalaeont. Soc. Publ. Ser.*, Bown, P.R. Ed., Chapman Hall, 1998, pp. 16–28.

Costa, E., Garces, M., Lopez-Blanco, M., et al., The Bartonian-Priabonian marine record of the eastern South Pyrenean foreland basin (NE Spain): a new calibration of the larger foraminifers and calcareous nannofossil biozonation, *Geologica Acta*, 2013, vol. 11, pp. 177–193.

Emel'yanov, E.M., Shimkus, K.M., Lisitsyn, A.P., et al., Geochemistry of Late Quaternary sediments in the Black Sea and peculiarities of its evolution, in *Geologiya morei i okeanov* (Geology of Seas and Oceans), Moscow: Nauka, 1977, no. 3, pp. 99–100.

Emel'yanov, E.M., The lithogeochemical aluminosilicate manganese carbonate region in the Gotland and Landsort basins, in *Osadkoobrazovanie v Baltiiskom more* (Sedimentation in the Baltic Sea), Moscow: Nauka, 1981, pp. 136–180.

Fornaciari, E., Agnini, C., Catanzariti, R., Rio, D., et al., Mid-latitude calcareous nannofossil biostratigraphy, biochronology and evolution across the middle to late Eocene transition, *Stratigraphy*, 2010, vol. 7, pp. 229–264.

Fornaciari, E. Raffi, I., et al., Biozonation and biochronology of Paleogene calcareous nannofossils from low and middle latitudes, *Newslett. Stratigraphy*, 2014, vol. 47, no. 2, pp. 131–181.

Gavrilov, Yu.O., Lithological signs of ancient earthquakes in the Cenozoic carbonaceous rocks of the northeastern Caucasus, *Geores. Geoenerg. Geopolit.*, 2016, vol. 13, no. 2, pp. 113–125.

Gavrilov, Yu.O., Reflection of seismic paleoevents in Mesozoic–Cenozoic terrigenous sequences of the northern Caucasus, *Lithol. Miner. Resour.*, 2017, no. 1, pp. 1–19.

Geologicheskie i bioticheskie sobytiya (Geological and Biotic Events), Krasheninnikov, V. A. and Akhmetiev, M. A., Eds., Moscow: Geos, 1998, part 2 (Late Eocene–Early Oligocene Geological and Biotic Events).

Hallberg, R.O., Paleoredox conditions in the Eastern Gotland Basin during the recent centuries, *Merentutkimusl. Julk*, 1974, no. 238, pp. 13–29.

Kholodov, V.N. and Nedumov, R.I., Geochemical criteria of the appearance of hydrosulfuric contamination in the water of ancient basin, *Izv. Akad. Nauk SSSR, Ser. Geol.*, 1991, no. 12, pp. 74–82.

Korolev, D.F., Role of iron sulfides in Mo accumulation in sedimentary rocks of the reductive zone, *Geokhimiya*, 1958, no. 4, pp. 22–45.

Krhovský, J., Adamowá, J., Hladikowc, J., and Maslowská, H., Paleoenvironmental changes across the Eocene-Oligocene boundary in the Ždanice and Pouzdrany units (Western Carpathians, Czechoslovakia), in *The long-term trend and orbitally forced changes in calcareous nannofossil assemblages*, Hamersmid, B. and Young, J., Eds., Prague: Knihovnička Zemn. Plynu Nafty, 1992, vol. 2, pp. 105–187

Martini, E., Standard Tertiary and Quaternary calcareous nannoplankton zonation, in *Proc. 2nd Plankt. Conf. Plankt. Microfossils,* Farinacci, A. Ed., Roma: Tecnoscienza, 1971, vol. 2, pp. 739–785.

Melinte-Dobrinescu, M.C. and Brustur, T., Oligocene-lower Miocene events in Romania, *Acta Palaeont. Roman.*, 2008, no. 6, pp. 203–215.

Melinte, M.C., Oligocene palaeoenvironmental changes in the Romanian Carpathians, revealed by calcareous nannofossils, *Studia Geol. Polon.*, 2005, vol. 124, pp. 1–12.

Metody izucheniya osadochnykh porod (Methods for the Study of Sedimentary Rocks), Strakhov, N.M., Ed., Moscow: Gosgeoltekhizdat, 1957.

Muzylev, N.G., Tabachnikova, I.P., and Voronina, A.A., The Early Oligocene stage of freshening in the Paratethys basins, *Izv. Akad. Nauk, Ser. Geol.*, 1992, no. 5, pp. 39–51.

Nagymarosy, A. and Voronina, A., Calcareous nannoplankton from the Lower Maikopian beds (Early Oligocene, Union of Independent States), in *Nannoplankton Research. Proc. Fourth INA Conf.*, Hamrsmid, B. and Young, J., Eds., Prague: Knihovnicka Zemn. Plynu Nafty, 1992, vol. 2, pp. 187–221.

Okada, H. and Bukry, D., Supplementary modification and introduction of code numbers to the low-latitude coccolith biostratigraphic zonation (Bukry, 1973, 1975), *Mar. Micropaleontol*, 1980, vol. 5, pp. 321–325.

Popov, S.V., Akhmetiev, M.A., Zaporozhets, N.I., et al., The Late Eocene–Early Oligocene history of the eastern Paratethys, *Stratigr. Geol. Korrelyatsiya*, 1993, vol. 1, no. 6, pp. 10–39.

Popov, S.V., Akhmetiev, M.A., Lopatin, A.V., et al., *Paleogeografiya i biogeografiya basseinov Paratetisa* (Paleogeography and Biography of Paratethys Basins), Moscow: Nauchn. Mir, 2009, part 1 (Late Eocene–Early Miocene).

Roban, D. and Melinte, M.C., Paleogene litho- and biostratigraphy of the NE Getic Depression (Romania), *Acta Palaeont. Roman.*, 2005, vol. 5, pp. 423–439.

Sachsenhofer, F.F., Popov, S.V., Akhmetiev, M.A., et al., The type section of the Maikop Group (Oligocene-Lower Miocene) at the Belaya River (North Caucasus): Depositional environment and hydrocarbon potential, *AAPG Bull.*, 2017, vol. 101, no. 3, pp. 289–319.

Sharafutdinov, V.F., *Geologicheskoe stroenie i usloviya formirovaniya miatlinskoi olistostromovoi tolshchi Severo-Vostochnogo Kavkaza* (Geological Structure and Formation Conditions of the Miatly Olistostrome Sequence in the northeastern Caucasus), Ufa: UGNTU, 2001.

Shatsky, N.S., Overthrust faults in the eastern Chernye gory region, northern Caucasia, *Byull. Mosk. O–va Ispyt. Prir., Otd. Geol.*, 1925, vol. 3, no. 3/4.

Shatsky, N.S. and Menner, V.V., The Paleogene stratigraphy in the eastern Caucasus, *Mosk. O–va Ispyt. Prir., Otd. Geol.*, *New Ser.*, vol. 35, 1927, pp. 39–60.

Somov, V.D., The Pshekh and Polbin horizons in the central and eastern Ciscaucasus, in *Tr. Grozn. NII*, 1965, no. 18, pp. 236–260.

Stolyarov, A.S., Paleogeography of the Ciscaucasus, Volga–Don, and southern Mangyshlak regions in the Late Eocene and Early Oligocene, *Byull. Mosk. O-va Ispyt. Prir., Otd. Geol.*, 1991, vol. 66, no. 4, pp. 64–80.

Stolyarov, A.S. and Ivleva, E.I., Solenovian rocks of the Lower Oligocene in the Ciscaucasia, Volga–Don and Mangyshlak regions (central part of the eastern Paratethys). Communication 1. Main lithological and structural features, *Lithol, Miner. Resour.*, 1999, no. 3, pp. 259–276.

Strougo, A., Faris, M., Haggag, M.A.Y., et al., Planktonic foraminifera and calcareous nannofossil biostratigraphy through the middle to late Eocene transition at Wadi Hitan, Fayum Province, Egypt, *Contr. Museum Paleont., Univ. Michigan*, 2013, vol. 32, pp. 111–138.

Tissot, B.P. and Welte, D.H., Petroleum Formation and Occurrence: A New Approach to Oil and Gas Exploration, Heidelberg: Springer, 1978. Translated under the title *Obrazovanie i rasprostranenie nefti*, Moscow: Mir, 1981.

Turekian, K.K. and Wedepohl, K.H., Distribution of elements in some major units of the earth's crust, *Geo-Mar. Lett.*, 1961, vol. 72, no. 2, pp. 175–192.

Tyson, R.V., *Sedimentary organic matter: organic facies and palynofacies*, London: Chapman Hall, 1995.

Vandenberghe, N., Hilgen, F.J., and Speijer, R.P., The Paleogene Period, in *The Geologic Time Scale*, Gradstein, F.M., Ogg, J.G., Schmitz, M. and Ogg, G., Eds., 2012. doi 10.1016/B978-0-444-59425-9.00028-7

Vinogradov, A.P., Average contents of chemical elements in the major types of igneous rocks in the Earth's crust, *Geokhimiya*, 1962, no. 7, pp. 555–571.

Voronina, A.A. and Popov, S.V., The Solenov horizon in the eastern Paratethys, *Izv. Akad. Nauk SSSR, Ser. Geol.*, 1984, no. 9, pp. 41–53.

Zhizhchenko, B.P., *Printsipy stratigrafii i unifitsirovannaya skhema deleniya kainozoiskikh otlozhenii Severnogo Kavkaza i smezhnykh oblastei* (Stratigraphic Principles and Unified Scheme for the Division of Cenozoic Sediments in the northern Caucasus and adjacent regions), Moscow: Gostoptekhizdat, 1958.

Translated by D. Sakya